Published in final edited form as:
Biochem Biophys Res Commun. 2008 February 22; 366(4): 932–937.

The RXRα C-terminus T462 is a NMR sensor for coactivator peptide binding

Jianyun Lu[a,*], **Minghe Chen**[a], **Gregory T. DeKoster**[b], **David P. Cistola**[c], and **Ellen Li**[a,b]

a *Department of Internal Medicine, Washington University School of Medicine, St. Louis, MO 63110*

b *Department of Biochemistry & Molecular Biophysics, Washington University School of Medicine, St. Louis, MO 63110*

c *Department of Biochemistry & Molecular Biology, Brody School of Medicine, East Carolina University, Greenville, NC 27858*

Abstract

The C-terminal activation function-2 (AF-2) helix plays a crucial role in retinoid X receptor alpha (RXRα)-mediated gene expression. Here, we report a nuclear magnetic resonance (NMR) study of the RXRα ligand-binding domain complexed with 9-cis-retinoic acid and a glucocorticoid receptor-interacting protein 1 peptide. The AF-2 helix and most of the C-terminal residues were undetectable due to a severe line-broadening effect. Due to its outstanding signal-to-noise ratio, the C-terminus residue, threonine 462 (T462) exhibited two distinct crosspeaks during peptide titration, suggesting that peptide binding was in a slow exchange regime on the chemical shift timescale. Consistently, the K_d derived from T462 intensity decay agreed with that derived from isothermal titration calorimetry. Furthermore, the exchange contribution to the ^{15}N transverse relaxation rate was measurable in either T462 or the bound peptide. These results suggest that T462 is a sensor for coactivator binding and is a potential probe for AF-2 helix mobility.

Keywords

RXRα; Activation; GRIP1; Coactivator; NMR; Isothermal titration calorimetry

Introduction

Retinoid X receptors (RXRα,β,γ) are members of the nuclear receptor (NR) superfamily of ligand-activated transcription factors. They function as either homodimers or obligate heterodimer partners with several other nuclear receptors and regulate target gene expression that governs diverse physiological processes from embryo- and organ-development to general metabolism [1].

The crystal structure of the unliganded RXRα LBD consists of 12 α-helices (H1 to H12) and one β-turn that are arranged into a three-layered antiparallel α-helical sandwich [2]. 9-cis-retinoic acid (9cRA) binding induces dramatic conformational changes including the AF-2 helix H12 partial unwinding and repositioning from an extended conformation to a folded one [3]. Compared to 9cRA binding, coactivator peptide binding induces only a small

*Corresponding author. Fax: 1-314-362-8959. E-mail: lujy@wustl.edu.

conformational change in the AF-2 helix [4]. Our previous high-resolution nuclear magnetic resonance (NMR) study [5] suggested that 9cRA binding stabilized the ligand-binding pocket and had an effect on the dimer interface. Surprisingly, the AF-2 helix only exhibited a moderate chemical shift perturbation and little changes in ^{15}N relaxation parameters induced by 9cRA binding.

To further characterize the dynamic property of the AF-2 helix in solution, we set out to investigate the binding interaction between the RXRα LBD-9cRA binary complex and a glucocorticoid receptor-interacting protein 1 (GRIP1) [6] peptide containing the second NR-interacting LXXLL box/motif [7], where L is leucine and X is any residue. We chose this peptide because it was previously co-crystallized in a number of RXRα LBD crystal structures [4]. Intriguingly, we found that the AF-2 helix and the C-terminal residues were no longer detectable in the ternary complex except for the C-terminus, T462. Our results suggest that T462 is a sensor for coactivator binding and is a potential probe for AF-2 helix mobility.

Materials and Methods

Materials

9cRA was purchased from Sigma-Aldrich (St. Louis, MO). The unlabeled and selectively L4-[^{15}N]-labeled GRIP1 NR box 2 peptide ^{686}KHKIL(1)HRL(4)L(5) and its L1A/L4A mutant were purchased with more than 95% purity from Biomolecules Midwest (Waterloo QDSS^{698}, IL). The L-Leucine-N-FMOC (^{15}N, 98%) used in the labeled peptide synthesis was purchased from Cambridge Isotope Laboratories (Andover, MA). The U-[^{2}H, ^{15}N]- and [^{2}H, ^{15}N, ^{13}C]-enriched RXRα LBDs were expressed in *Escherichia coli* BL21-DE3 bacteria, isolated by Talon affinity chromatography, digested by thrombin to remove the N-terminal His_6 tag, and finally purified by gel filtration chromatography as described [5].

NMR Sample Preparation

The preparation of 0.7–1.0 mM ternary complex samples for resonance assignments and relaxation measurements was as described [5] with the following modification. A two-fold molar excess of the peptide over the LBD was added to the sample following 9cRA addition, and another one molar equivalent amount of the peptide was added to the sample prior to the final exchange. For NMR titration, 10, 25 or 100 mM peptide-DMSO-d_6 stock solution was added to 0.3–0.4 mM U-[^{2}H, ^{15}N]-enriched RXRα LBD-9cRA binary complex (the holo-LBD) stock solution. The final 500-μl-NMR samples contained 0.27 mM binary complex and 0.0, 0.14, 0.27, 0.40, 0.54, 1.5, 3.0, or 5.0 mM GRIP1 peptide, respectively. The total volume of the DMSO-d_6 was kept at 20 μl in all samples to minimize the solvent effect.

NMR Spectroscopy

All NMR experiments were carried out at 25 °C on either 600- or 700-MHz four-channel Varian Inova spectrometers equipped with pulsed-field gradient triple resonance probes. All experiments employed the transverse relaxation-optimized spectroscopy (TROSY) scheme [8] unless specified otherwise. For sequence-specific resonance assignments and backbone ^{15}N relaxation measurements, data collection, processing and analysis were as described [5]. For NMR titration, the 2-dimensional (2D) ^{1}H-^{15}N heteronuclear single quantum correlation (HSQC) spectra were recorded on the 700-MHz spectrometer, with 10500 and 1983 Hz spectral width and 672 and 116 complex data points in the ^{1}H and ^{15}N dimension, respectively, 64 scans per free induction decay, 1.8 s relaxation delay, and a total of 8 h for each spectrum. The K_d was calculated in the SigmaPlot program (SPSS, Chicago, IL) by fitting the intensities to a single-site-per-monomer binding equation $I_i/I_f = 1 - (1 - F_{min})(-b - \sqrt{(b^2 - 4ac)})/2a$, where $a = [P_t]/K_d$, $b = -1 - ([P_t] + [L_{t,\,i}])/K_d$, $c = [L_{t,\,i}]/K_d$, $[P_t]$ was the total LBD concentration, $[L_{t,\,i}]$ was the total peptide concentration at the ith titration, F_{min} was the

minimal fractional intensity, I_f, and I_i, were the titer-free and the *i*th titration intensities, respectively.

Isothermal Titration Calorimetry (ITC)

The experiment was carried out using a Microcal (Amherst, MA) OMEGA isothermal titration calorimeter at 25°C. The NMR buffer was used to prepare both 50 μM holo-LBD solution and 2.0 mM GRIP1 peptide solution to minimize heat of dilution. A total of 96 μl of the peptide solution were added in 24 identical injections to the reaction cell containing either 1.3 ml of the holo-LBD solution or buffer as control. After correcting for heat of peptide dilution, the integrated peak intensities were fit to a multiple-identical-sites-per-LBD binding model to calculate the binding constant ($1/K_d$), stoichiometric ratio (n) and heat of binding (ΔH) using the Origin software provided by the manufacturer. Two independent measurements were conducted to estimate the uncertainties.

Results

Sequence-Specific Resonance Assignments of the RXRα LBD-9cRA-GRIP1 Peptide Ternary Complex

The sequence-specific $^{13}C^{\alpha}$, ^{13}CO and $^{13}C^{\beta}$ resonance assignments have been established for 198 of 240 LBD residues in the ternary complex using a suit of 3D- and 4D-triple resonance experiments as described [5]. The backbone amide crosspeaks of 182 residues have been identified from a total of 226 expected residues after excluding the 14 proline-residues. The chemical shift values have been deposited in BioMagResBank with accession No. BMRB15219. Compared to the binary complex, we could detect residue L279 in helix H3 and F346 in helix H7 that were missing in the binary complex. But we could no longer detect residues D444-T445 and L451-M461 encompassing the AF-2 helix (Fig. 1A), which were observable in the binary complex.

Line-Broadening Effect on the AF-2 Helix Induced by Peptide Binding

To examine the binding interaction between the LBD and the peptide, we performed peptide titration on the holo-LBD at different molar ratios and monitored crosspeak changes in the 2D HSQC spectra. Residue K284 in helix H3, which forms one end of a charge clamp [9] for coactivator binding (Fig. 1A), exhibited two inversely attenuated crosspeaks corresponding to the peptide-free and -bound states that did not move during titration (Fig. 1B). In general, most of the residues in the vicinity of coactivator binding surface changed in the same fashion as K284. In contrast, residue A457 at the C-terminal end of the AF-2 helix, which plays a key role for coactivator binding [4,9], exhibited only the attenuated peptide-free crosspeak that did not move during titration (Fig. 1C). Other residues in the AF-2 helix and the C-terminal region changed in the same fashion as A457 except for the C-terminus T462. These data suggest that peptide binding can exert a line-broadening effect on the AF-2 helix and the C-terminal region.

To assess the role of ligand binding, we performed titration on the apo-LBD (unliganded) under the same condition. It was intriguing that residues K284 (Fig. 1D) and A457 (Fig. 1E) exhibited changes similar to those of the respective residues in the holo-LBD at a much higher peptide-to-LBD ratio (≥ 5.6). These data suggest that high peptide-to-LBD ratios can overcome the loss of ligand binding and exert a line-broadening effect on the AF-2 helix and the C-terminal region.

Peptide Binding is in a Slow Exchange Regime on the Chemical Shift Timescale

In the HSQC spectrum recorded on the holo-LBD, the signal intensity of the C-terminus T462 was almost 20-fold higher than those in the LBD core including helices H1-H10, as revealed

by a histogram in Fig. 2A. Like the residues mentioned above, T462 exhibited two inversely but unevenly attenuated crosspeaks that did not move during titration (Fig. 2B). Together, these data suggest that peptide binding is in a slow exchange regime on the chemical shift timescale.

It is well known that, in the slow exchange regime, the peptide on-off exchange contribution is negligible and the measured peak intensity directly correlates with the concentration of the peptide-free or peptide-bound state [10]. Thus, we fit the intensity decay curve of T462 to a single-site-per-LBD binding equation, and the resulting peptide dissociation constant K_d was 16 ± 2 μM (Fig. 2C). In order to independently validate this approach, we performed ITC measurements on peptide binding to the holo-LBD at the same temperature (Supplementary Fig. 1). The resulting heat of binding ΔH was −7.9 ± 0.5 kcal/mol, the stoichiometric ratio n was 0.91 ± 0.04, and the K_d was 10 ± 3 μM, which closely agreed with that derived from T462.

Using T462 as the NMR probe, we estimated that the K_d for GRIP1 peptide binding to apo-LBD was 0.25 ± 0.08 mM (Fig. 2C). As a negative control, we performed titration on the holo-LBD using a peptide with double mutations in the NR box AXXAL, which was shown to abolish NR-binding capacity [7]. The resulting K_d was 1.5 ± 0.4 mM (Fig. 2C), suggesting that the mutant did not bind to the holo-LBD as expected. Of note, data at two high concentrations were not available for wild type peptide titration on the holo-LBD due to severe precipitation. Thus, these data suggest that although the apo-LBD may weakly associate with the GRIP1 peptide, 9cRA can dramatically enhance the binding affinity by ~16 fold.

Line-Broadening Effect on T462 is Due to Exchange on the Millisecond (ms) Timescale

To confirm the line-broadening effect exhibited in the peptide-bound state of T462 (Fig. 2B), we performed ^{15}N transverse relaxation time T_2 measurement on a 1.0 mM ternary complex using a non-TROSY scheme and compared the result with those of the apo- and holo-LBD [5]. In the ternary complex, the T_2 of T462 decreased by 3- and 4-fold relative to the apo- and holo-LBD, respectively (Fig. 3A). Because applied B_1 field strength can attenuate the exchange contribution to the transverse relaxation rate R_2 ($R_2 = 1/T_2$) [11], we performed R_2 measurements at two different B_1 field strengths (1000 and ~0 Hz). The ΔR_2 was negligible for T462 in either the apo-or holo-LBD (Fig. 3B), whereas it was substantial in the ternary complex measured in both 500-MHz (11-fold) and 700-MHz (7.6-fold) static magnetic field strengths. Thus, this result suggests that the line-broadening effect on T462 is due to exchange on the ms timescale.

Exchange Line Broadening on the Bound Peptide

To test whether the peptide could also sense exchange on the ms timescale, we obtained a selectively L4-[^{15}N]-labeled GRIP1 peptide and performed the same set of experiments on the labeled peptide without and with equal molar amount of the holo-LBD in natural isotopic abundance. The peptide exhibited a single sharp peak (Fig. 4A) and two broad peaks (Fig. 4B) in the absence and presence of the holo-LBD, respectively. The ΔR_2 was negligible in the absence of the holo-LBD, and was substantial but not identical to that of T462 in the presence of the holo-LBD (Fig. 4C). Thus, exchange on the ms timescale contributes to the line-broadening effect on the bound peptide.

Discussion

The AF-2 helix plays a crucial role in RXR activation. Here, the NMR titration analysis showed that the difficulty of detecting the AF-2 helix and most of the C-terminal residues in the ternary complex was the result of a line-broadening effect. The ^{15}N transverse relaxation rate analysis showed that exchange on the ms timescale contributed to the line-broadening effect on both T462 and L4 of the bound peptide. Due to its outstanding signal-to-noise ratio, the C-terminus

T462 exhibited two distinct crosspeaks that did not move during titration. This is similar to the findings on most residues in the vicinity of coactivator-binding surface, suggesting that peptide binding is in a slow exchange regime on the chemical shift timescale. The finding that the K_d derived from T462 intensity decay agreed with that derived from the ITC measurement is consistent with the above conclusion. Therefore, these results suggest that T462 is a NMR sensor for coactivator peptide binding.

The titration analysis on T462 showed that 9cRA could dramatically enhance peptide binding affinity by ~16 fold, which is in close agreement with the increase (~13 fold) induced by a synthetic RXR agonist [12] and with the increased transcriptional output induced by 9cRA [13]. It was surprising to detect weak binding between the apo-LBD and GRIP1 peptide since RXR is a ligand-activated transcription factor. Furthermore, affected residues were primarily located on the coactivator-binding surface (Fig. 1D), suggesting that a small fraction of the apo-LBD might be in the active conformation. Whether the peptide itself or with the help of residual LBD-bound bacterial fatty acids induces or stabilizes the active conformation remains to be clarified.

The findings that GRIP1 peptide binding is in the slow exchange regime on the chemical shift timescale and that the line-broadening effect is most profound in the AF-2 helix lead us to speculate that conformational exchange may contribute to line broadening of the AF-2 helix. It is difficult to directly measure such a conformational exchange due to the loss of AF-2 resonances in the ternary complex. Similar effect on the AF-2 helix of a PPARγ LBD ternary complex has been reported [14], suggesting that AF-2 helix line broadening may be a general phenomenon of a NR LBD-ligand-coactivator peptide ternary complex in solution. It is important to determine whether this phenomenon can be extended to a RXR heterodimer. We recently demonstrated that it is feasible to monitor residue-specific structural and dynamic changes of a RXR LBD heterodimer in response to ligand binding in solution [15].

In summary, our study demonstrates that T462 is a NMR sensor for coactivator peptide binding, and is a potentially useful probe for measuring AF-2 helix mobility on multiple timescales (from picosecond to millisecond) and for studying the mechanism of allosteric ligand activation in RXR heterodimers.

Supplementary Material

Refer to Web version on PubMed Central for supplementary material.

Acknowledgements

We thank Mr. John Monsey and Dr. Alexander Koslov for assistance in ITC. This work was supported by grants from the National Institutes of Health (NIH) DK59501 (E. Li), Washington University Digestive Diseases Research Core Center (DK 52574), a pilot/feasibility award (J. Lu) from the Washington University Center for Human Nutrition (DK 56341). Spectra were collected at the Washington University Molecular Biophysics NMR laboratory and the High Resolution NMR Service Facility in Chemistry, which are funded in part by the NIH through NCRR shared Instrument Grants RR13874 and RR015715, respectively.

References

1. Desvergne B. RXR: from partnership to leadership in metabolic regulations. Vitam Horm 2007;75:1–32. [PubMed: 17368310]
2. Bourguet W, Ruff M, Chambon P, Gronemeyer H, Moras D. Crystal structure of the ligand-binding domain of the human nuclear receptor RXR-alpha. Nature 1995;375:377–382. [PubMed: 7760929]
3. Egea PF, Mitschler A, Rochel N, Ruff M, Chambon P, Moras D. Crystal structure of the human RXRα ligand-binding domain bound to its natural ligand 9-cis retinoic acid. EMBO J 2000;19:2592–2601. [PubMed: 10835357]

4. Egea PF, Mitschler A, Moras D. Molecular recognition of agonist ligands by RXRs. Mol Endocrinol 2002;16:987–997. [PubMed: 11981034]
5. Lu J, Cistola DP, Li E. Analysis of ligand binding and protein dynamics of human retinoid X receptor alpha ligand-binding domain by nuclear magnetic resonance. Biochemistry 2006;45:1629–1639. [PubMed: 16460010]
6. Hong H, Kohli K, Tgivedi A, Johnson DL, Stallcup MR. GRIP1, a novel mouse protein that serves as a transcriptional coactivator in yeast for the hormone binding domains of steroid receptors. Proc Natl Acad Sci USA 1996;93:4948–4952. [PubMed: 8643509]
7. Voegel JJ, Heine MJ, Tini M, Vivat V, Chambon P, Gronemeyer H. The coactivator TIF2 contains three nuclear receptor-binding motifs and mediates transactivation through CBP binding-dependent and -independent pathways. EMBO J 1998;17:507–519. [PubMed: 9430642]
8. Pervushin K, Riek R, Wider G, Wüthrich K. Attenuated T2 relaxation by mutual cancellation of dipole-dipole coupling and chemical shift anisotropy indicates an avenue to NMR structures of very large biological macromolecules in solution. Proc Natl Acad Sci USA 1997;94:12366–12371. [PubMed: 9356455]
9. Nolte RT, Wisely GB, Westin S, Cobb JE, Lambert MH, Kurokawa R, Rosenfeld MG, Willson TM, Glass CK, Milburn MV. Ligand binding and co-activator assembly of the peroxisome proliferator-activated receptor-γ. Nature 1998;395:137–143. [PubMed: 9744270]
10. Ernst, RR.; Bodenhausen, G.; Wokaun, A. Principles of nuclear magnetic resonance in one and two dimensions. 1. Oxford University Press; New York: 1987.
11. Palmer AG III, Kroenke CD, Loria JP. Nuclear magnetic resonance methods for quantifying microsecond-to-millisecond motions in biological macromolecules. Methods Enzymol 2001;339:204–238. [PubMed: 11462813]
12. Pogenberg V, Guichou JF, Vivat-Hannah V, Kammerer S, Perez E, Germain P, de Lera AR, Gronemeyer H, Royer CA, Bourguet W. Characterization of the interaction between retinoic acid receptor/retinoid X receptor (RAR/RXR) heterodimers and transcriptional coactivators through structural and fluorescence anisotropy studies. J Biol Chem 2005;280:1625–1633. [PubMed: 15528208]
13. Schulman IG, Juguilon H, Evans RM. Activation and repression by nuclear hormone receptors: hormone modulates an equilibrium between active and repressive states. Mol Cell Biol 1996;16:3807–3813. [PubMed: 8668198]
14. Chen S, Johnson BA, Li Y, Aster S, McKeever B, Mosley R, Moller DE, Zhou G. Both coactivator LXXLL motif-dependent and -independent interactions are required for peroxisome proliferator-activated receptor γ (PPARγ) function. J Biol Chem 2000;275:3733–3736. [PubMed: 10660518]
15. Lu J, Chen M, Stanley SE, Li E. Effect of heterodimer partner RXRα on PPARγ activation function-2 helix in solution. Biochem Biophys Res Commun. 200710.1016/j.bbrc.2007.10.143

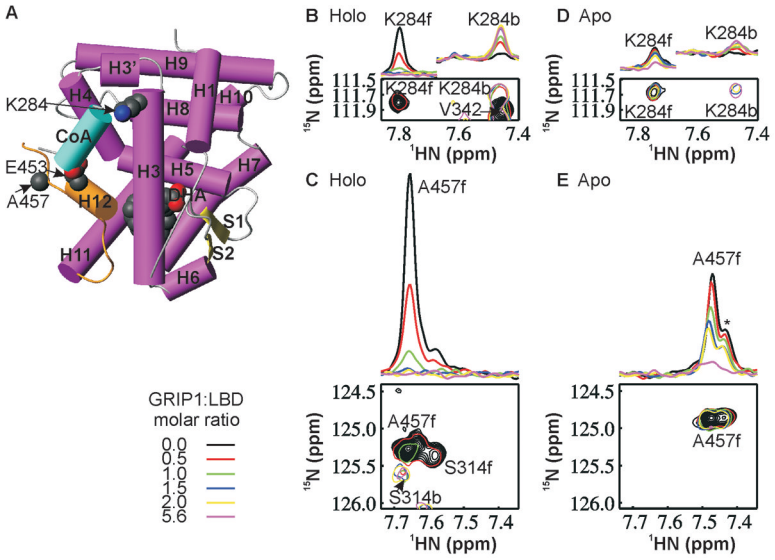

Fig. 1.

Line-broadening effect on the AF-2 helix induced by GRIP1 peptide binding. (A) The crystal structure of the RXRα LBD-docosahexaenoic acid (DHA)-GRIP1 peptide (CoA) ternary complex (PDB: 1MV9) showing the side chains of the charge clamp residues K284 and E453 and the AF-2 residue A457. Color schemes: orange, regions showing the line-broadening effect; magenta, helices H1-H11; yellow, strands S1 and S2; gray, coil; cyan, CoA; gray, red and blue balls, C, O and N atoms, respectively. (B–E) Overlay of expanded regions of 2D-HSQC spectra recorded on 0.27 mM either RXRα LBD (apo) (D, E) or its 9cRA binary complex (holo) (B, C) titrated with 0.0 (black), 0.14 (red), 0.27 (green), 0.40 (blue), 0.54 (yellow), and 1.5 (magenta) mM GRIP1 peptide. For clarity, only the peptide-free spectrum is shown in full contour levels and the rest are shown in baseline level. 1D slices were taken at the peaks of K284 (B, D) and A457 (C, E) in the peptide-free (f) and -bound (b) states. An asterisk designates a minor peak of A457.

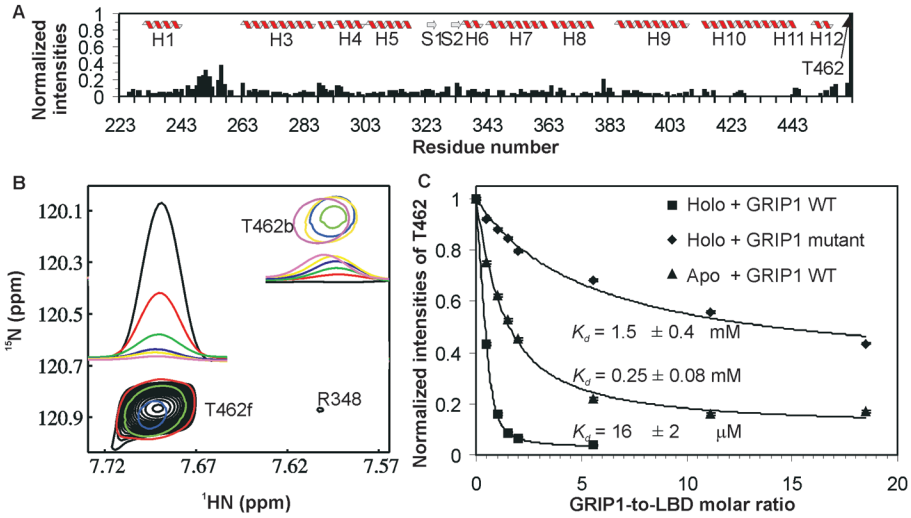

Fig. 2.

The intensity of the RXRα C-terminus T462 is a sensitive measure of coactivator binding affinity. (A) Histogram of intensities measured in the 2D-HSQC spectra of the holo-LBD and normalized to that of T462, excluding overlapping residues. Ribbon diagrams are the secondary structure in the crystal structure. (B) Overlay of the expanded regions in the 2D-HSQC spectra for T462, as described in Fig. 1. (C) Normalized intensity decay of the peptide-free T462 crosspeak (T462f) against the wild type or mutant GRIP1 peptide concentration for the apo- and holo-LBD. Solid lines are the calculated curves obtained by fitting the data to the one-site per LBD binding equations.

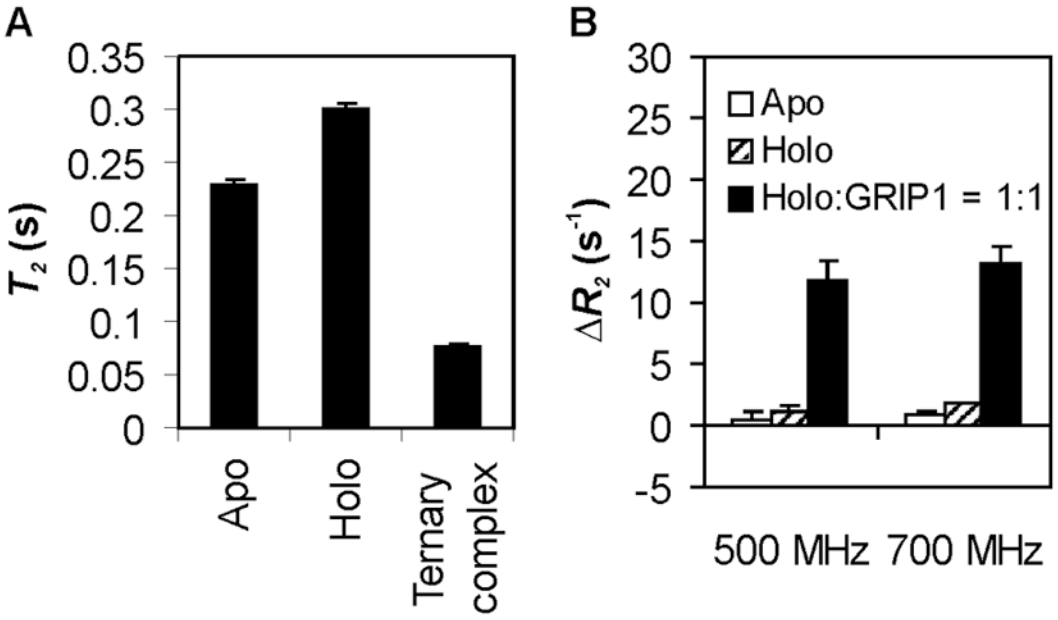

Fig. 3.

Line-broadening effect on T462 is due to exchange on the millisecond (ms) timescale. (A) Backbone ^{15}N transverse relaxation times (T_2) of T462 in the apo- and holo-LBD and the ternary complex measured in a 700-MHz spectrometer. (B) Exchange contribution ΔR_2 to the transverse relaxation rate of T462 in the apo- and holo-LBD and the ternary complex measured in both 500-and 700-MHz spectrometers.

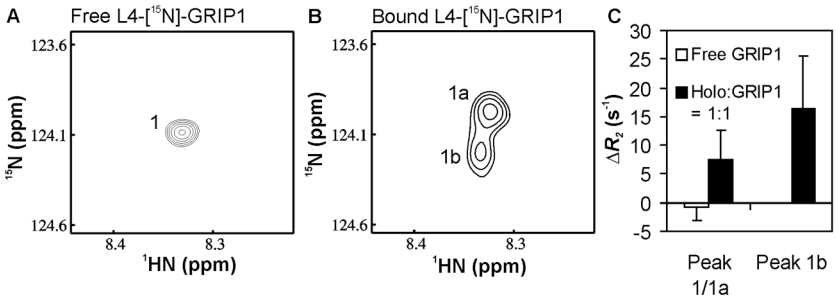

Fig. 4.

Exchange line broadening on the bound peptide. (A) 2D-HSQC spectrum of 1.2 mM L4-[^{15}N]-labeled GRIP1 peptide recorded at 700-MHz spectrometer. (B) 2D-HSQC spectrum of 0.7 mM labeled peptide in the presence of 0.7 mM holo-LBD in natural isotopic abundance. (C) Exchange contribution ΔR_2 to the transverse relaxation rate of the L4 residue in the LBD-free and LBD-bound peptides measured in the 700-MHz spectrometer.